Proceedings World Geothermal Congress 2020+1
Reykjavik, Iceland, April - October 2021

Analysis of Recuperative Transcritical Organic Rankine Cycle Using Mixture Working Fluids in Low Enthalpy Geothermal

Jui-Ching HSIEH[a], Shao-Min Zheng[b], Bo-Heng LEE[c], David T.W. LIN[d], Chun-Ping JEN[e]

[a] Department of Mechanical Engineering, National Chin-Yi University of Technology, Taichung, Taiwan

E-mail address: jchsieh@ncut.edu.tw

[b] Department of Mechanical Engineering, National Chin-Yi University of Technology, Taichung, Taiwan

E-mail address: a0975527473@gmail.com

[c] Green Energy and Environment Research Laboratories, Industrial Technology Research Institute, Hsinchu, Taiwan

E-mail address: bohenglee@itri.org.tw.

[d] Institute of Mechatronic System Engineering, National University of Tainan, Tainan, Taiwan

E-mail address: davidlin7991@gmail.com

[e] Department of Mechanical Engineering, National Chung Cheng University, Chiayi, Taiwan

E-mail address: chunping.jen@gmail.com

Keywords: Transcritical organic rankine cycle, zeotropic mixtures, recuperator

ABSTRACT

The low-enthalpy heat in geothermal fluids is extracted by using a binary cycle and is converted into electricity. Conventional Organic Rankine Cycles (ORCs) are used widely in low-enthalpy geothermal power plants as an effective solution to convert low-grade heat into power. However, conventional ORCs are characterized by high exergy destruction during heat transfer in the evaporator and condenser. The irreversibility of evaporator and condenser, and exergy loss of the heat source can be reduced by employing zeotropic mixtures and transcritical organic Rankine cycles (TRCs). A thermodynamic analysis model of TRC adopting recuperator associated with mixtures has been developed. This model was employed to investigate feasibility of the mixture R600a/R134a instead of R245fa/R134a in the low-enthalpy heat. Therefore, the mixtures are investigated by the first and second law efficiencies of thermodynamic, exergy destruction and specific power at various inlet expander temperatures and pressures. The results indicate that the optimal mole fraction corresponding to the maximal specific power is dramatically and unsignificantly affected by the inlet temperature and inlet pressure of the expander, respectively. Meanwhile, the maximal specific power occurred at temperature difference between $T_{exp,in}$ and T_{cri} approaching 40 °C under effects of condensing temperature glide. The peak value of the first law effficiecny is occurred at pure R245fa and R600a. The second law efficiency and the specific power are increased considerably by increasing inlet temperature and inlet pressure of the expander. The comparsions show the similar trend in terms of condensing pressure and heat transfer rate of recuperator, nevertheless the significant difference is in the condensing temperature glide. By the recuperator, the total exergy destruction can be reduced, especially for $T_{exp,in} \geq 170$ °C.

1. INTRODUCTION

By the growing industrialization, energy consumption has sharply increased over past decades, which led to environmental problems such as acid rain, ozone layer depletion and global warming. Methods of improving energy efficiency are crucial for energy efficiency policies and environmental protection. Organic Rankine Cycle (ORC) is one of effective methods to recovery low-grade waste heat to generate electricity. Tchanche *et al.* [1] listed the ORC power plants operating, which capacity ranges from 125 kW to 6 MW. Many authors have studied ORC. The focus of the survey was on the selection of organic fluids [2-4] and parameter optimization [5-7]. Among several types of renewable energy sources, geothermal energy seems to be the most attractive energy source because it is stable, unaffected by weather conditions, and easily utilized by traditional technologies. However, most geothermal resources are obtained at temperatures below 150 °C and are therefore referred to as "low temperature" or "low enthalpy" geothermal resources [8]. In addition, the use of low temperature geothermal energy can be achieved by using a binary device. Approximately 44 % of existing units are binary plants in the geothermal due to their lower average capacity, which production is less than 10 % of the world's geothermal [9].

The performance comparison between sub- and transcritical organic Rankine cycle has been investigated at various heat sources [10-15]. Xu et al. [10] examined effect of heat source temperature, critical temperature and evaporating pressure on sub- and supercritical organic Rankine cycle. They found that the net power output for supercritical ORC decreases rapidly with the rise of evaporation pressure when the flue gas temperature is near to the working fluid's critical temperature. Meanwhile, the maximum net power output was appeared if the heat source temperature was approximately 25-40°C higher than the working fluid's critical temperature. Braimakis et al. [11] found that the use of mixtures instead of pure fluids can have a significantly positive effect on the cycle performance under specific waste heat temperature. Compared to subcritical ORC, the supercritical ORC can improve exergetic efficiency [15].

From the viewpoint of environmental protection, carbon dioxide is a promising natural working fluid in binary cycles. Moreover, CO_2 and its mixtures have been studied by researchers in the transcritical cycle [16-20]. Wu et al. [17] found that CO_2-based mixtures were unsuitable for transcritical power cycles at low cooling water temperatures, except R161/CO_2 and R152a/CO_2. Wang and Dai [18] studied the TRC with CO_2 and ORC with different organic fluids as the bottoming cycles. They found that the performance of the CO_2-TRC was superior to that of the ORC at lower compressor pressure ratios. Dai et al. [19] found that CO_2-based zeotropic mixtures can improve the thermal performance and lower the operation pressure compared with pure CO_2. Pan et al. [20] indicated that thermal oil outlet temperatures were affected by heating pressure and mass fraction associated with R290/CO_2 mixture in TRC. Vélez et al. [21, 22] investigated the use of a low temperature heat source for power generation through a CO_2 transcritical power cycle. Their theoretical results revealed the irrevseribilities of evaporator and condenser were reduced with input pressure due to the rise in the pump outlet temperature of fluid to cause an increase in the exergetic efficiency. Cayer et al. [23] found that a pressure of approximately 13.5 MPa maximized the thermal and exergetic efficiencies in CO_2 transcritical cycle without regenerator at pressure range from 9 to 15 MPa. Although the CO_2-based mixtures have been investigated in the literature, the associated system costs were found to be markedly high because the supercritical pressure of CO_2 is higher than that of the other organic mixtures.

As expected from previous works [11, 14, 24] the internal heat exchanger (IHE), namely recuperator, can increase the thermal and exergy efficiency, but the exhaust temperature of heat source was higher than that of the corresponding non-recuperative cycle [25]. Consequently, the ORC adapting recuperator configuration is useful to increase output power at constant thermal power input. However, the geothermal fluid controlled at fixed mass flowrate could be not increased output power by recuperator [25]. Additionally, the studies [25, 26] illustrated for dry and isentropic fluids ORC adopting recuperator could be recover more sensible heat. Wang and Zhao [26] indicated for zeotropic mixtures introducing a recuperator to ORC system can also notably increase thermal efficiency because of effect of the mixture's temperature glide during condensing. However, the evidence on performance associated with temperature glide of the mixtures introducing recuperator is limited.

Although hydrofluorocarbons refrigerants, namely R245a and R134a, are popular and widely used as working fluid in ORC system, they have high GWP. Hydrocarbon refrigerants (for instance R600a), which with low GWP and higher flammability, are environmentally friendly, non-toxic and non-ozone-depleting. The objective of the present study was investigated to feasibility of the relative low GWP fluid, namely R600a, instead of R245fa in the TRC with R134a-based mixtures at heat source inlet temperature ranged from 160 to 210 °C.

2. THEORETICAL ANALYSIS

The schematic diagram of TRC system is shown in Figure 1. The mixtures R245fa/R134a and R600a/R134a were used as working fluids to investigate effects of system parametric and recuperator on TRC performance. Figure 2 shows the T-s diagram for TRC system, which indicates the temperature glide of the working fluid vapor in the condenser. The temperature glide provided better temperature match between cooling water and working fluid during condensing process. It is meaning that the irreversibility was lower during working fluid condensing process to improve system efficiency. In the present study, the properties of the working fluid were referred to the REFPROP 9.0 [27] and analysis system was developed by using computer program in MATLAB. The given parameters of TRCs associated with the mixtures and heat source are listed in Table 1. The system assumptions were given as below:

- The system in steady state.
- Ignored pressure drop of the evaporator, the condenser and the pipes.
- Ignored heat loss of the each component and the pipes.

For the TRC system the pumps pressurize the working fluid to a supercritical state, resulting in a high pressure difference between the evaporator and condenser. However, the working fluid pumps consume considerable power from the system generator. To understand the weighting of the consumed power on the output power of the system, the first and second law efficiency of thermodynamic are estimated using the following equations:

$$\dot{W}_{pump} = \dot{m}_f(h_2 - h_1) \tag{1}$$

$$\dot{W}_{exp} = \dot{m}_f(h_4 - h_3) \tag{2}$$

$$\dot{W}_{net} = \dot{W}_{exp} - \dot{W}_{pump} \tag{3}$$

$$\eta_I = \frac{\dot{W}_{net}}{\dot{Q}_h} \tag{4}$$

$$\Delta\dot{E}_h = \dot{m}_h[(h_{h,in} - h_{h,out}) - T_0(S_{h,in} - S_{h,out})] \tag{5}$$

$$\eta_{II} = \frac{\dot{W}_{net}}{\Delta\dot{E}_h} \tag{6}$$

where $\dot{W}_{net}$ is the difference between the shaft power produced by the expander and the power consumed by the pump of working fluid. The total heat transfer rate in the evaporator is a product of the mass flow rate of the working fluid and enthalpy difference between the outlet and inlet of evaporator.

To consider the specific power, we express the net output power per unit mass flow rate of the heat source as follows:

$$\zeta = \frac{\dot{P}_{net}}{\dot{m}_{hs}} \tag{7}$$

where $\dot{P}_{net}$ is

$$\dot{P}_{net} = (\dot{W}_{exp} \cdot \varepsilon_{g,m}) - \frac{\dot{W}_{pump}}{\varepsilon_{g,m}} \tag{8}$$

The efficiency of the main components and the system was evaluated using thermodynamic and energy balance equations. The main design points and components are displayed in Figure 2. The mathematical model for each component is listed in Table 1.

Table 1: The mathematical model of the component for simple and recouperative TRC.

	Simple	Recouperative
$\dot{I}_{eva}$, Ω_{eva}	$\dot{I}_{eva} = \dot{m}_f T_o(S_3 - S_2) + \dot{m}_h T_o(S_{h,out} - S_{h,in})$ $\dot{Q}_h = \dot{m}_f(h_3 - h_2)$ $\Omega_{eva} = \frac{\dot{I}_{eva}}{\Delta\dot{E}_h}$	$\dot{I}_{eva} = \dot{m}_f T_0(S_3 - S_7) + \dot{m}_h T_o(S_{h,out} - S_{h,in})$ $\dot{Q}_h = \dot{m}_f(h_3 - h_7)$ $\Omega_{eva} = \frac{\dot{I}_{eva}}{\Delta\dot{E}_h}$
$\dot{I}_{exp}$, Ω_{exp}	$\dot{I}_{exp} = \dot{m}_f T_o(S_4 - S_3)$ $\Omega_{exp} = \frac{\dot{I}_{exp}}{\Delta\dot{E}_h}$	$\dot{I}_{exp} = \dot{m}_f T_o(S_4 - S_3)$ $\Omega_{exp} = \frac{\dot{I}_{exp}}{\Delta\dot{E}_h}$
$\dot{I}_{cond}$, Ω_{cond}	$\dot{I}_{cond} = \dot{m}_f T_0(S_1 - S_4) + \dot{m}_c T_0(S_{c,out} - S_{c,in})$ $\Omega_{cond} = \frac{\dot{I}_{cond}}{\Delta\dot{E}_h}$	$\dot{I}_{cond} = \dot{m}_f T_0(S_1 - S_6) + \dot{m}_c T_0(S_{c,out} - S_{c,in})$ $\Omega_{cond} = \frac{\dot{I}_{cond}}{\Delta\dot{E}_h}$
$\dot{I}_{pump}$, Ω_{pump}	$\dot{I}_{pump} = \dot{m}_f T_o(S_2 - S_1)$ $\Omega_{pump} = \frac{\dot{I}_{pump}}{\Delta\dot{E}_h}$	$\dot{I}_{pump} = \dot{m}_f T_o(S_2 - S_1)$ $\Omega_{pump} = \frac{\dot{I}_{pump}}{\Delta\dot{E}_h}$
$\dot{I}_{rec}$, Ω_{rec}	NA	$\dot{I}_{rec} = \dot{m}_f T_0(S_7 + S_6 - S_2 - S_4)$ $\Omega_{rec} = \frac{\dot{I}_{rec}}{\Delta\dot{E}_h}$

The normalized exergy destruction of the TRC system can be summarized as follows:

$$\Omega_{total} = \Omega_{pump} + \Omega_{eva} + \Omega_{exp} + \Omega_{cond} + \Omega_{rec} \tag{9}$$

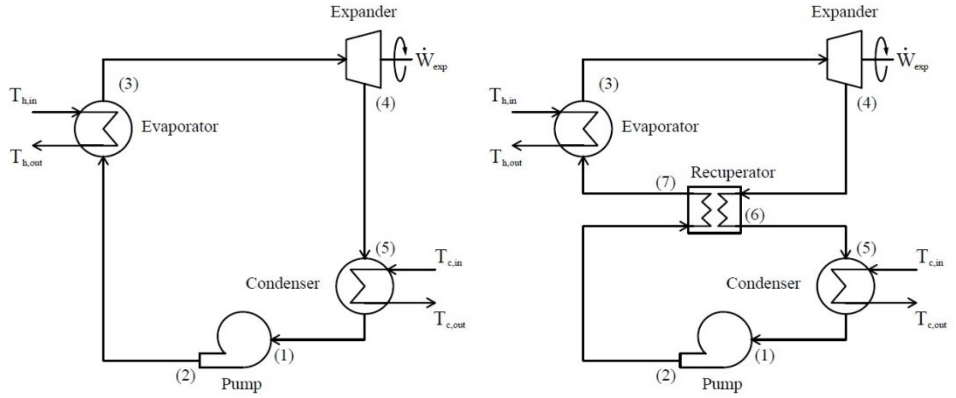

(a) (b)

Figure 1: Schematic of (a) simple and (b) recuperative TRC.

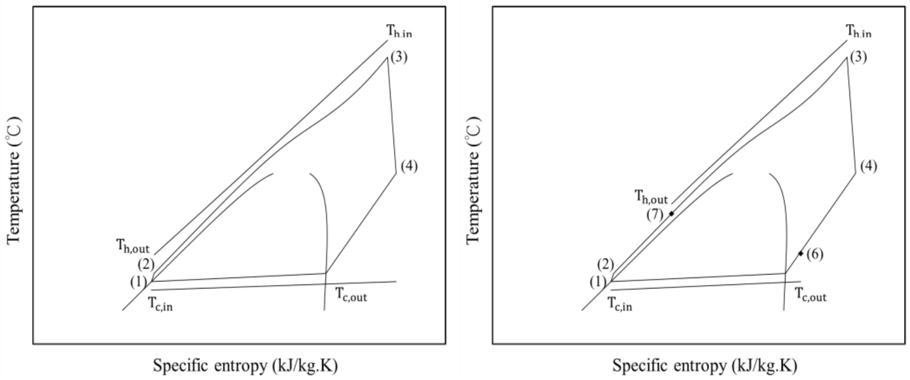

(a) (b)

Figure 2: T-s diagram of mixture (a) in simple and (b) recuperative TRC.

Table 2: Given parameters of TRC.

Turbine isentropic efficiency	η_{exp}	80 %
Pump isentropic efficiency	η_{pump}	65 %
Recuperator effectiveness	ε_{rec}	80 %
Generator/motor efficiency	$\varepsilon_{g,m}$	90 %
Temperature difference of pinch point in the evaporator	$\Delta T_{pp,eva}$	5 K
Temperature difference of pinch point in the condenser	$\Delta T_{pp,cond}$	5 K
Inlet temperature of the expander	$T_{exp,in}$	150 – 200 °C
Inlet pressure of the expander	$P_{exp,in}$	4.1 - 6.6 MPa
Temperature of geothermal fluid	$T_{h,in}$	160 – 210 °C
Mass flow rate of geothermal fluid	$\dot{m}_h$	30 kg/s
Inlet temperature of cooling source	$T_{c,in}$	32 °C
Ambient temperature	T_0	32 °C

RESULTS AND DISCUSSION

The present study was carried out theoretical analysis to investigate feasibility of the organic fluids R600a/R134a instead of R245fa/R134a in the TRC. The first and second law efficiencies of thermodynamic, and specific power affected by $T_{exp,in}$ and mole fraction of the mixtures at constant inlet pressure of expander are shown in Figures 3 and 4. The results show that the specific power and first law efficiency are notably increased with an increase of $T_{exp,in}$. The line are not shown at high mole fraction of the front fluid at low $T_{exp,in}$ due to small tempeature difference between the T_{cri} and $T_{exp,in}$ to cause droplet accumulation during pressure drop. For the TRC system, the critical point is the crucial property of the working fluid because the working fluid must be in the supercritical state before entering the expander. To avoid droplet accumulation owing to a drop in pressure, the inlet temperature of the working fluid should be sufficiently higher than the critical temperature to ensure that the working fluid remains in the superheated state during expansion. It is worth noated that the peak value of the first law efficiency is occurred at pure R245fa and R600a. However, the two peaks value of the second law efficiency and specific power are observed at high inlet temperature of the expander. The reason for the corrsponding peak value is the condensing temperature glide approaching the temperature difference between the inlet and outlet of cooling source. For R245fa/R134a and R600a/R134a the optimal mole fraction corresponding to the maximal specific power at various inlet temperatures are listed in Table 3. The mole fraction of R245fa and R600a with high critical temperature is low at $T_{exp,in} \leq 180$ and 170 °C, respectively. This is because of the maximal specific power occurred at temperature difference between $T_{exp,in}$ and T_{cri} approaching 40 °C under effects of condensing temperature glide. Furthermore, for R245/R134a the first and second law efficiencies, and specific power are higher than those of R600a/R134a.

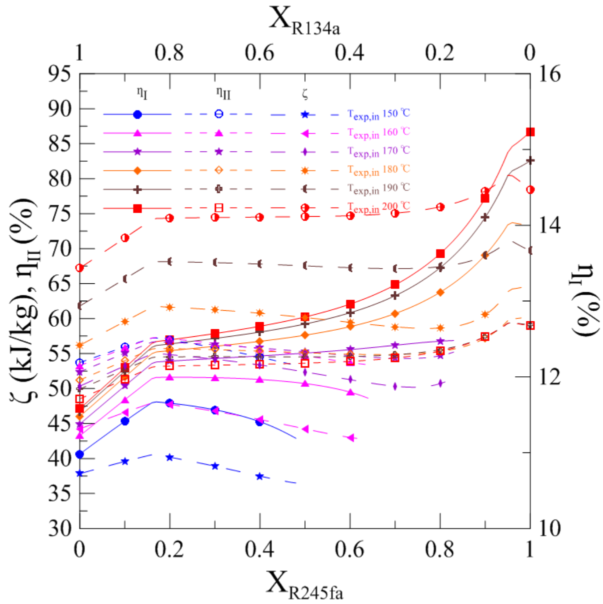

Figure 3: Effect of the inlet temperature of expander on the first and second law efficiencies of thermodynamic, and specific power of R245fa/R134a at $P_{exp,in}$=5.6 MPa.

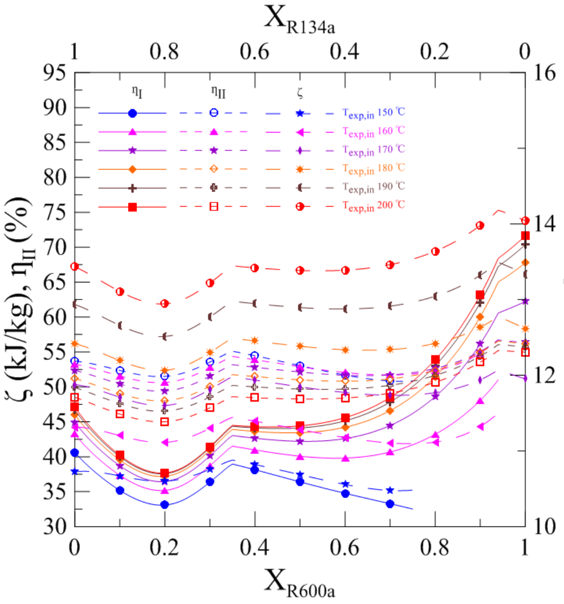

Figure 4: Effect of the inlet temperature of expander on the first and second law efficiencies of thermodynamic, and specific power of R600a/R134a at $P_{exp,in}$=5.6 MPa.

Table 3: Mole fraction of the mixtures corresponding to the maximal specific power at various $T_{exp,in}$ ($P_{exp,in}$= 5.6 MPa).

$T_{exp,in}$		150°C	160°C	170°C	180°C	190°C	200°C
R245fa/R134a	ζ	40.53	47.97	55.02	61.72	71.06	80.49
	X	0.17/0.83	0.17/0.83	0.17/0.83	0.17/0.83	0.95/0.05	0.95/0.05
R600a/R134a	ζ	39.53	45.65	51.45	60.07	67.82	75.3
	X	0.35/0.65	0.35/0.65	0.35/0.65	0.94/0.06	0.94/0.06	0.94/0.06

Figures 5 and 6 illurate the first and second law efficiencies of thermodynamic, and the specific power affected by the inlet pressure of the expander. The results show that the efficiencies and specific power increased with an increase of $P_{exp,in}$ at constant $T_{exp,in}$. This is because of the entropy of evaporator outlet and expander outlet declined with the operating pressure. Meanwhile, the mole fraction of the mixtures at peak values of the corresponding second law efficiency and specific power are unsignificantly affected by $P_{exp,in}$.

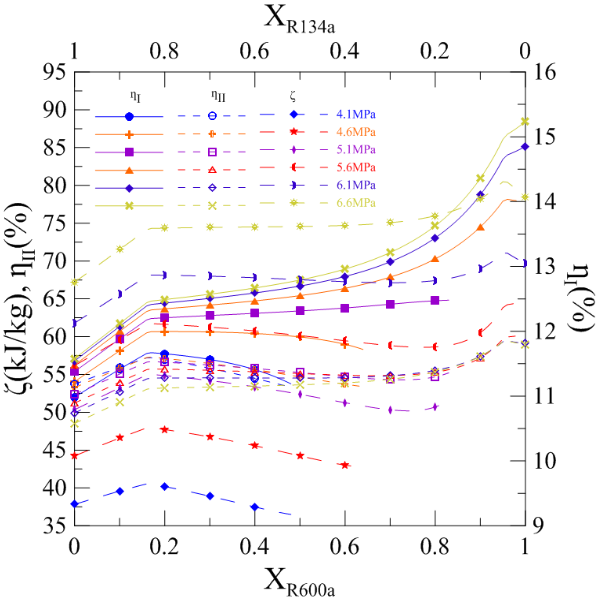

Figure 5: Effect of the inlet pressure of expander on the first and second law efficiencies of thermodynamic, and specific power of R245fa/R134a at $T_{exp,in}$=200 °C.

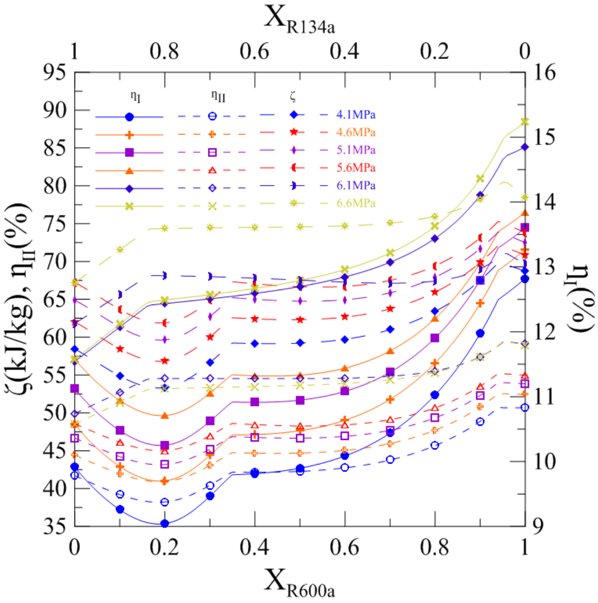

Figure 6: Effect of the inlet pressure of expander on the first and second law efficiencies of thermodynamic, and specific power of R600a/R134a at $T_{exp,in}$=200 °C.

To investigate effect of condensing temperature glide on the recuperator, the heat transfer rate of the recuperator at constant effectiveness is shown in Figures 7 and 8. The comparsions show the similar trend in terms of condensing pressure (P_{cond}) and heat transfer rate of recuperator (Q_{rec}), nevertheless the significant difference is in the condensing temperature glide. The results show that the heat transfer rate of recuperator is increased with the condensing pressure. It is meant that the heat transfer rate in recuperator of the fluids with low critical temperature is higher than that of the fluids with high critical temerature.

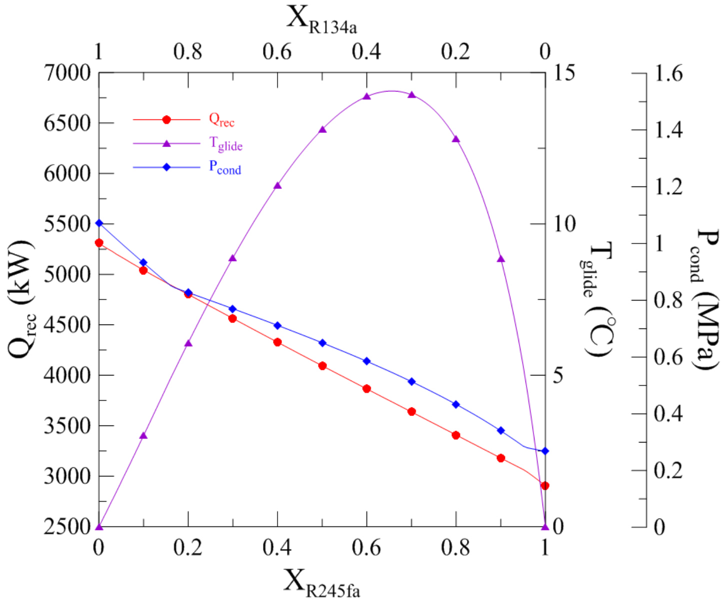

Figure 7: The heat transfer rate of R245fa/R134a with recuperator effectiveness of 80% at $T_{exp,in}$=200 °C and $P_{exp,in}$=5.6 MPa.

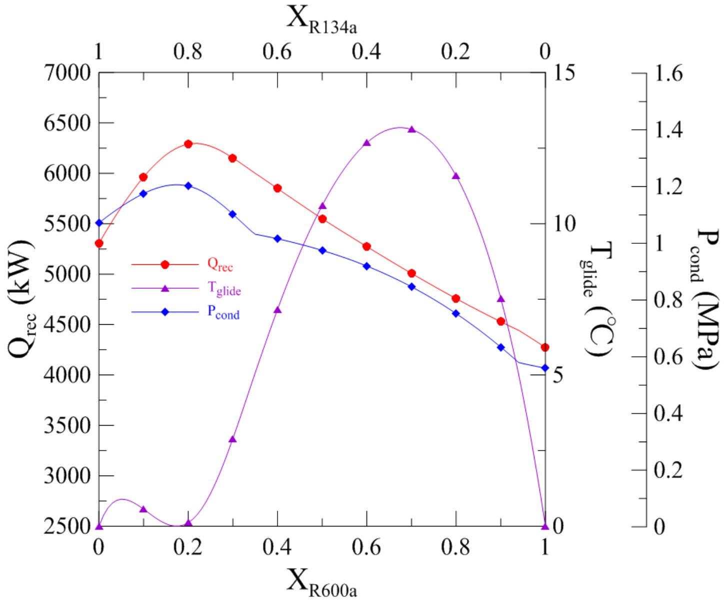

Figure 8: The heat transfer rate of R600a/R134a with recuperator effectiveness of 80% at $T_{exp,in}$= 200 °C and $P_{exp,in}$=5.6 MPa.

Figures 9 and 10 show that effect of TRC adopting recuperator on the normalized exergy destruction at various $T_{exp,in}$ and $P_{exp,in}$. The results illurate that the total exergy destruction is considerably reduced by recuperator resulted from a decrease of the mass flow rate of cooling source and entropy difference between outlet and inlet of condenser in refrigerant side. Meanwhile, for non-recuperative TRC the exergy destruction is decreased with an increase of inlet pressure of the expander. This is because of the the irreversibilities of the evaporator and condenser reduced by the operating pressure, when $T_{exp,in}$ ≥160 °C. However, for recuperative TRC the exergy destruction dramatically declines first and then increases with an increase in expander inlet pressure, especially when $T_{exp,in}$ ≤190 °C.

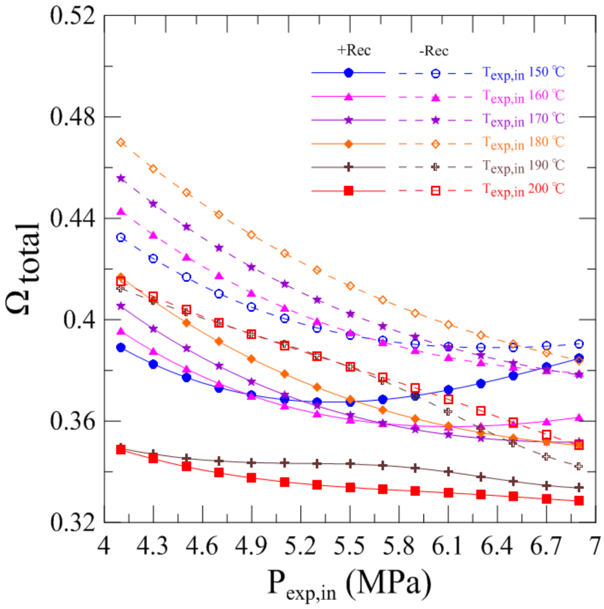

Figure 9: Effect of the inlet temperature and pressure of expander on total normalized exergy destruction of R245fa/R134a.

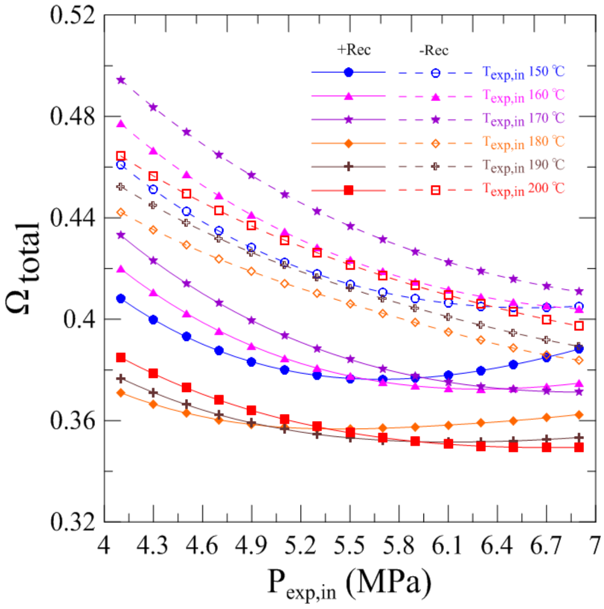

Figure 10: Effect of the inlet temperature and pressure of expander on total normalized exergy destruction of R600a/R134a.

CONCLUSIONS

In the present study, the mixtures (R245fa/R134a and R600a/R134a) with optimal mole fraction corresponding to the maximal specific power was examined by thermodynamic method at various inlet expander pressures and temperatures to investigate feasibility of the other organic fluids, R600a, instead of HFC, namely E245fa, in the TRC with mixtures. The conclusions were summarized as follows:

1. The optimal mole fraction of the mixtures corresponding to the maximal specific power is considerably and unsignificantly affected by $T_{exp,in}$ and $P_{exp,in}$, respectively. The pure R245fa and R600a have the maximal value of the first law efficiency. Furthermore, for R245/R134a the first and second law efficiencies, and specific power are higher than those of R600a/R134a.
2. The efficiencies and specific power are increased with $T_{exp,in}$ and $P_{exp,in}$. However, the second law efficiency is slightly affected by $T_{exp,in}$.
3. The similar trend in terms of condensing pressure and heat transfer rate of recuperator, nevertheless the significant difference is in the condensing temperature glide. The heat transfer rate in recuperator of the fluids with low critical temperature is higher than that of the fluids with high critical temerature.
4. The total exergy destruction is considerably reduced by recuperator resulted from a decrease of the mass flow rate of cooling source and entropy difference between outlet and inlet of condenser in refrigerant side.

ACKNOWLEDGMENTS

The financial support provided to this study by the Ministry of Science and Technology of the Republic of China under NO. MOST 108-2221-E-167 -007 -MY3 is gratefully acknowledged.

REFERENCES

1. Tchanche, B.F., Lambrinos, Gr, Frangoudakis, A., Papadakis, G., 2011, Low-grade heat conversion into power using organic Rankine cycles – A review of various applications, *Renew. Sustain. Energy Rev.*, vol. 15: p. 3963-3979.
2. Chen, H., Goswami, D.Y., Stefanakos, E.K., 2010, A review of thermodynamic cycles and working fluids for the conversion of low-grade heat, *Renew. Sustain. Energy Rev.*, vol. 14: p. 3059-3067.
3. Lai, N.A., Wendland, M., Fischer, J., 2011, Working fluids for high-temperature organic Rankine cycles, *Energy*, vol. 36: p. 199-211.
4. Saleh, B., Koglbauer, G., Wendland, M., Fischer, J., 2007, Working fluids for low-temperature organic Rankine cycles, *Energy*, vol. 32: p. 1210-1221.
5. Ayachi, F., Ksayer, E.B., Zoughaib, A., Neveu, P., 2014, ORC optimization for medium grade heat recovery, *Energy*, vol. 68: p. 47-56.
6. Dai, Y., Wang, J., Gao, L., 2009, Parametric optimization and comparative study of organic Rankine cycle (ORC) for low grade waste heat recovery, *Energy Convers. Manag.*, vol. 50: p. 576-582.
7. Schuster, A., Karellas, S., Aumann, R., 2010, Efficiency optimization potential in supercritical Organic Rankine Cycles, *Energy*, vol. 35: p. 1033-1039.
8. Barbier, E., 2002, Geothermal energy technology and current status: an overview, *Renew. Sust. Energ.*, Rev. 6: p. 3-65.
9. Bertani, R., 2012, Geothermal power generation in the world 2005–2010 update report, *Geothermics*, vol. 41: p. 1-29.
10. Xu H, Gao N, Zhu T, Investigation on the fluid selection and evaporation parametric optimization for sub- and supercritical organic Rankine cycle. Enrgy 2016;96:59-68.
11. Braimakis K, Preißinger M, Brüggemann D, Karellas S, Panopoulos K. Low grade waste heat recovery with subcritical and supercritical Organic Rankine Cycle based on natural refrigerants and their binary mixtures. Energy 2015;88:80–92.
12. H. Xu, N. Gao, T. Zhu, Investigation on the fluid selection and evaporation parametric optimization for sub- and supercritical organic Rankine cycle. Energy 96 (2016) 59-68.
13. M. Li, J. Wang, S. Li, X. Wang, W. He, Y. Dai, Thermo-economic analysis and comparison of a CO2 transcritical power cycle and an organic Rankine cycle. Geothermics 50 (2014) 101-111.
14. Algieri A, Morrone P. Comparative energetic analysis of high-temperature subcritical and transcritical Organic Rankine Cycle (ORC): A biomass application in the Sibari district. Appl therm Eng 2012;36:236–24.
15. S. Zhang, H. Wang, T. Guo, Performance comparison and parametric optimization of subcritical Organic Rankine Cycle (ORC) and transcritical power cycle system for low-temperature geothermal power generation. Applied Energy 88 (2011) 2740-2754.
16. Chen H, Goswami DY, Rahman MM, Stefanakos EK. Energetic and exergetic analysis of CO_2- and R32-based transcritical Rankine cycles for low-grade heat conversion. Appl Energy 2011;88:2802–08.
17. Wu C, Wang SS, Jiang X, Li J. Thermodynamic analysis and performance optimization of transcritical power cycles using CO_2-based binary zeotropic mixtures as working fluids for geothermal power plants. Appl Therm Eng 2017;115:292–304.
18. Wang X, Dai Y. Exergoeconomic analysis of utilizing the transcritical CO_2 cycle and the ORC for a recompression supercritical CO_2 cycle waste heat recovery: A comparative study. Appl Energy 2016;170:193–207.
19. Dai B, Li M, Ma Y. Thermodynamic analysis of carbon dioxide blends with low GWP (global warming potential) working fluids-based transcritical Rankine cycles for low-grade heat energy recovery. Energy 2014;64:942–52.
20. Pan L, Wei X, Shi W. Performance analysis of a zeotropic mixture (R290/CO2) for trans-critical power cycle. Chinese Journal of Chemical Engineering 2015;23:572-77.
21. Vélez F, Segovia J, Chejne F, Antolín G, Quijano A, Martín MC. Low temperature heat source for power generation exhaustive analysis of a carbon dioxide transcritical power cycle. Energy 2011;36:5497-5507.
22. Vélez F, Chejne F, Antolín G, Quijano A. Theoretical analysis of a transcritical power cycle for power generation from waste energy at low temperature heat source. Energy Conversion and Management 2012;60:188-95.
23. Gayer E, Galanis N, Desilets M, Nesteddine H, Roy P. Analysis of a carbon dioxide transcritical power cycle using a low temperature source. Applied Energy 2009;86:1055-63.
24. M. Li, J. Wang, S. Li, X. Wang, W. He, Y. Dai, Thermo-economic analysis and comparison of a CO2 transcritical power cycle and an organic Rankine cycle. Geothermics 50 (2014) 101-111.
25. D. Maraver, J. Royo, V. Lemort, S. Quoilin, Systematic optimization of subcritical and transcritical organic Rankine cycles (ORCs) constrained by technical parameters in multiple applications. Applied energy 117 (2014) 11-29.
26. X.D. Wang, L. Zhao, Analysis of zeotropic mixtures used in low-temperature solar Rankine cycles for power generation. Energy 83 (2009) 605-613.
27. Lemmon EW, Huber ML, McLinden MO. NIST Standard Reference Database 23: Reference Fluid Thermodynamic and Transport Properties REFPROP, Version 9.1, National Institute of Standards and Technology, Standard Reference Data Program, Gaithersburg, USA, 2013.

NOMENCLATURE

h	specific enthalpy (kJ/kg)
$\dot{I}$	exergy destruction (kW)
$\dot{m}$	mass flow rate (kg/s)
P	pressure (MPa)
$\dot{P}$	electrical power (kW)
Q	heat transfer rate (kW)
S	specific entropy (kJ kg^{-1} K^{-1})

T	temperature (°C)
$\dot{W}$	mechanical shaft power (kW)
X	mole fraction of mixture (%)

Greek letters

ε, η	efficiency (%)
ζ	specific power (kJ/kg)
$\Delta\dot{E}$	available exergy (kW)
ΔT	temperature difference (K)
Ω	exergy destruction rate

Subscript

0	environment state
1-7	state point
c	cooling source
c,in/c,out	cooling source inlet/outlet
cond	condenser/condensation
evap	evaporator/evaporation
exp	expander
f	working fluid
g	generator
glide	glide
h	heat source
h,in/h,out	heat source inlet/outlet
I/II	first/second law of thermodynamics
in/out	inlet/outlet
m	motor
net	net
pp	pinch point
pump	pump
rec	recuperator
total	total